Microstructure of Ionomers Based on Sulfonated Block Copolymers of Polystyrene and Poly(ethylene-*alt*-propylene)

Sudhir Mani,[†,⊥] R. A. Weiss,[*,†] C. E. Williams,[‡] and S. F. Hahn[§]

Department of Chemical Engineering and Polymer Science Program, University of Connecticut, Storrs, Connecticut 06269; Laboratoire des Fluides Organises, CNRS URA 792, College de France, 11 Place Marcelin-Berthelot, 75231 Paris Cedex 05, France; and Corporate Research—Materials Research and Synthesis Laboratory, The Dow Chemical Company, Midland, Michigan 48674

Received January 25, 1999; Revised Manuscript Received March 23, 1999

ABSTRACT: Block copolymer ionomers were prepared by lightly sulfonating the polystyrene (PS) blocks of diblock and triblock copolymers of PS and poly(ethylene-*alt*-propylene) (PEP), followed by neutralization of the sulfonic acid groups with either sodium or zinc. The block copolymers contained between 10 and 50 wt % PS, and as the PS content increased, the mesophase texture varied from PS spheres to hexagonal-close-packed (hcp) PS cylinders to alternating PS and PEP lamellae. The sulfonation level was varied from 1 to 17 mol % of the styrene repeat units, which provided a range of functionalization (N_S) of between 2 and 9 sulfonate groups per molecule. The microstructure was analyzed by small-angle X-ray scattering (SAXS) and dynamic mechanical thermal analysis (DMTA). An ion-rich microphase formed within the PS microdomains, and that hindered the development of a well-ordered block texture. Sulfonation of a diblock copolymer containing ca. 20 wt % PS resulted in a transition of the block microphase texture from a hcp to lamellar. The order-to-disorder transition temperature, T_{ODT}, of the block copolymer was relatively insensitive to the choice of the cation, and T_{ODT} increased as N_S increased.

Introduction

Block copolymers and ionomers represent two classes of polymers that exhibit the phenomenon of microphase separation. In block copolymers, microphase formation is driven by the thermodynamic immiscibility of the dissimilar homopolymer blocks where the covalent bond between the blocks prevents bulk phase separation. Self-assembled, periodic structures on a size scale of 10−50 nm, such as body-centered-cubic-packed (bcc) spheres, hexagonal-close-packed (hcp) cylinders, alternating lamellae, and more complex phases, have been theoretically predicted and experimentally observed.[1] The specific texture achieved with a particular system depends on the copolymer composition, molecular weight, copolymer architecture, and the magnitude of the repulsive interactions between the chemically dissimilar blocks as characterized by a temperature-dependent χ-interaction parameter. An entropically driven order-to-disorder transition (ODT) can occur at elevated temperature and is sometimes preceded by order-to-order transitions (OOTs) between specific mesophase textures.[2,3]

Ionomers exhibit microphase separation of ion-rich aggregates as a result of electrostatic interactions between the charged moieties.[4−6] In this case, the characteristic size of the microphase is 1−5 nm. It has been predicted that high temperatures should destabilize the ionic aggregation and produce an ODT,[7] but in general, this is not observed at accessible temperatures for random copolymer ionomers.

Several research groups have prepared ion-containing block copolymers.[8−16] Block copolymer ionomers prepared by lightly sulfonating the polystyrene end blocks of a poly(styrene-*b*-(ethylene-*co*-butylene)-*b*-styrene) (SEBS) triblock copolymer exhibited two distinct microstructures: one on a size scale of 20−30 nm due to the block copolymer texture and the other on a size scale of 3−4 nm due to the ionic aggregation within the polystyrene microdomains.[11−16] A thermally induced ODT of the ionic aggregates was observed in those materials.[14,16]

Our previous research on block copolymer ionomers[11−16] was restricted to a single block copolymer architecture, i.e., a triblock SEBS containing ∼30 wt % polystyrene, which had a mesophase texture of short, poorly developed cylindrical PS domains. In this paper, we describe the microstructure and microphase behavior of block copolymer ionomers based on diblock and triblock copolymers covering a range of textures including spherical and cylindrical polystyrene microdomains and alternating lamellae of polystyrene and a polyolefin rubber. These materials were prepared by lightly sulfonating the polystyrene (PS) blocks in diblock and triblock copolymers of PS and poly(ethylene-*alt*-propylene) (PEP). The copolymer composition was varied between ca. 10 and 50 wt % PS. Different degrees of sulfonation and cations were examined. Synchrotron small-angle X-ray scattering (SAXS) was used to characterize the room-temperature block microphase texture and study the morphology of the ionic microphase. The temperature-induced microphase transitions were probed using dynamic mechanical thermal analysis (DMTA).

Experimental Details

Ionomer Synthesis and Sample Preparation. Diblock and triblock copolymers of PS and PEP, hereafter denoted as SEP and SEPS, respectively, were prepared by anionic polymerization of block copolymers of PS and polyisoprene (PI) followed by selective hydrogenation of the PI blocks. Details of the synthesis are described elsewhere.[17] The nominal number-average molecular weight of all the block copolymers was 50 000 Da; see Table 1. Ionomers were prepared by lightly

* To whom correspondence should be addressed.
† University of Connecticut.
‡ College de France.
§ The Dow Chemical Company.
⊥ Present address: Unilever Research, Bebington, Wirral L63 3JW (U.K.).

10.1021/ma9900986 CCC: $18.00
Published on Web 04/28/1999

Table 1. Molecular Characteristics of the Block Copolymer Ionomers

designation[a]	w_{PS}[b]	M_n, Da[c]	M_w/M_n[c]	s[d]	N_S[e]
2.5M-SEP20	0.203	54 000	1.04	2.55	2.7
5.5M-SEP20	0.203	54 000	1.04	5.5	5.8
1.9M-SEP35	0.356	52 000	1.03	1.9	3.4
2M-SEP50	0.504	52 000	1.04	2.05	5.2
17.2M-SEPS9	0.090	54 900	1.16	17.25	8.2
5.1M-SEPS21	0.215	49 300	1.08	5.1	5.2
6.4M-SEPS21	0.215	49 300	1.08	6.4	6.5
8.7M-SEPS21	0.215	49 300	1.08	8.7	8.9
3.6M-SEPS50	0.508	50 000	1.12	3.65	8.8

[a] M = H^+, Na^+, or Zn^{2+}. [b] Weight fraction of PS in the parent block copolymer, determined by ^1H NMR. [c] Determined for the parent block copolymer by GPC. [d] Mole percent of styrene sulfonated (average of values from titration and elemental sulfur analysis). [e] $N_S = (s/100)(w_{PS})M_n/104)$ = average number of sulfonate groups per chain.

sulfonating the PS blocks using acetyl sulfate in 1,2-dichloroethane at 50−55 °C following the procedure used to sulfonate SEBS[15] with the following two changes: (1) *n*-hexane was used as a cosolvent with 1,2-dichloroethane in a proportion of 1:3 (v/v) to dissolve the block copolymers with low PS weight fraction, i.e., for $w_{PS} \approx 0.10$, and (2) the sulfonated polymer was recovered by precipitation in an excess of cold methanol instead of steam-stripping. The extent of sulfonation was determined by titration of the free-acid derivative to a phenolphthalein end point in a mixed solvent of toluene/methanol (9/1 v/v) using standardized solutions of methanolic sodium hydroxide. Elemental sulfur analysis (Galbraith Laboratories, Knoxville, TN) was used to verify the sulfonation level for most samples. Sodium and zinc salts were prepared by fully neutralizing the free-acid derivatives in a toluene/methanol (9/1 v/v) mixed solvent with a methanolic solution of sodium hydroxide and zinc acetate dihydrate, respectively.

The characteristics of the ionomers are summarized in Table 1. The samples are denoted by *s*M-SEP*x* or *s*M-SEPS*x*, where "*s*" and "M" represent the sulfonation level in mole percent of styrene sulfonated and the cation (H, Na, or Zn). The parent block copolymers are denoted as "SEP*x*" for diblock copolymers and "SEPS*x*" for triblock copolymers, where "*x*" is the weight percent PS.

Solution-cast samples were prepared by casting 10% (w/v) solutions of the block copolymer ionomer in toluene/methanol (9/1 v/v) onto partially covered glass dishes over a period of 7 days. The cast films were peeled off the glass and dried to constant weight at 50 °C under vacuum. The ionomer films were annealed at 100 °C for 24 h under vacuum except for the 17.2M-SEPS9 samples, which were annealed at 70 °C for 24 h. Solution-cast samples of the parent block copolymers were prepared from toluene solutions using the procedure described in ref 17.

Small-Angle X-ray Scattering (SAXS). SAXS measurements were made on a beamline D22 at the DCI-LURE synchrotron radiation source in Orsay, France. A description of the beamline optics is available elsewhere.[18] The intensity of the scattered X-rays was recorded using a gas-filled position-sensitive proportional counter. Different experimental conditions were used to measure the scattering from the block and ionic microphases: (1) an X-ray wavelength, λ, of 0.1377 nm and a sample-to-detector distance (SDD) of 1.252 or 1.522 m, or $\lambda = 0.1458$ nm and SDD = 1.560 m for the block microstructure, and (2) $\lambda = 0.1377$ nm and SDD = 0.474 m for the ionic microstructure. The SAXS data were corrected for parasitic scattering, incident beam decay, sample absorption, and thermal background, and the data are presented in relative units. Conversion to absolute intensity requires a simple multiplicative factor. The beamline optics were such that desmearing corrections were not required.

The scattering peak positions quoted in this paper were defined as the middle of the full width at half-maximum. For the sharper, narrower peaks, the precision was of the order of one pixel of the detector. When the signal-to-noise was poor, e.g., for the broader, less intense peaks, several different representations of the data (i.e., I vs q, ln I vs q, and q^2I vs q, where I is the scattering intensity, q is the scattering vector $= 4\pi(\sin\theta)/\lambda$, θ is one-half the scattering angle, and λ is the X-ray wavelength) were used to confirm that there was a peak. For those peaks, the relative precision of q_{max} was poorer, probably of the order of 4−5 pixels.

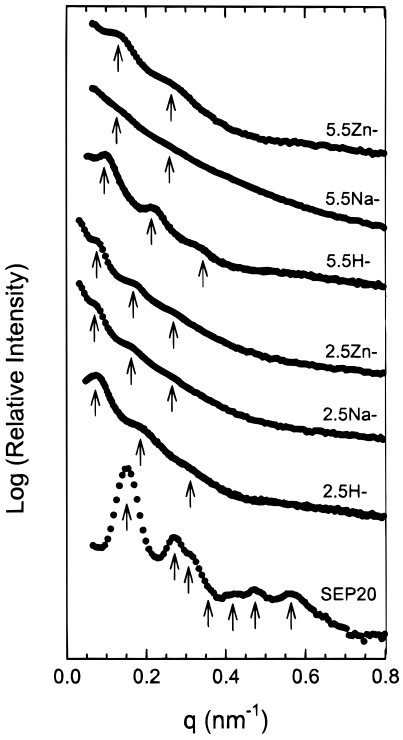

Figure 1. SAXS curves for the block copolymer microphase for SEP20 and *s*M-SEP20 ionomers. Vertical arrows indicate maxima of the structure factor, $S(q)$.

Dynamic Mechanical Thermal Analysis (DMTA). Dynamic storage and loss moduli, G' and G'', were measured with a Polymer Laboratories' PL-DMTA Mk II using a shear-sandwich test fixture (7 mm diameter shear studs), heating rates between 0.2 and 1.0 °C/min, strains of 0.5−2.0%, and a frequency of 0.1 Hz. A nitrogen atmosphere was used to minimize oxidative degradation of the samples.

Results and Discussion

Block Microstructure. Sulfonation greatly perturbed the block microphase texture of the polymers. Figure 1 shows the SAXS curves for the *s*M-SEP20 diblock ionomer series. The curves are plotted as the logarithm of relative scattered intensity versus scattering vector, q. The vertical arrows in Figure 1 indicate the maxima in the structure factor. The scattering vector at the position of the first maximum, q^*, was used to estimate the characteristic dimension, D, of the microstructure using Bragg's law, $D = 2\pi/q^*$, and the values of D are given in Table 2.

The ratios q_m/q^*, where m is the order of the scattering maximum (i.e., $m = 1, 2, 3, ...$) and $q^* \equiv q_1$, were used to determine the microphase texture associated with each SAXS curve. For the SAXS curve of the parent SEP20 block copolymer, $q_m/q^* = 1, \sqrt{3}, 2, \sqrt{7}, ...$, which corresponds to hcp PS cylinders[19] in a PEP matrix. The *s*M-SEP20 ionomers, however, had a lamellar (lam) texture, as evidenced by the values of $q_m/q^* \approx 1, 2, 3$. The poor resolution of the SAXS maxima indicates that the lamellar order was imperfect.

The origin of the change in texture of the block copolymer from hcp to lam upon sulfonation is most

Table 2. Microstructure Parameters and Microphase Transition Temperatures for Diblock Copolymer Ionomers

polymer	block microphase texture[a]	D (D_i)[b] (nm)	$T_{g,\,PS}$[c] (°C)	$T_{g,i}$[c] (°C)	T_{ODT}[c] (°C)
SEP20	hcp cyl	40.4	95	*d*	325
2.5H-SEP20	lamellae	85.4	*e*	*e*	*e*
2.5Na-SEP20	lamellae	79.6	*e*	*e*	*e*
2.5Zn-SEP20	lamellae	73.4	*e*	*e*	*e*
5.5H-SEP20	lamellae	64.0	95	135	335
5.5Na-SEP20	lamellae	44.7	95	160	315
5.5Zn-SEP20	lamellae	47.2	90	150	325
SEP35	lamellae	53.1	*e*	*e*	*e*
1.9H-SEP35	lamellae	56.7	*e*	*e*	*e*
1.9Na-SEP35	lamellae	44.7	*e*	*e*	*e*
1.9Zn-SEP35	lamellae	53.1	*e*	*e*	*e*
SEP50	lamellae	49.9	*e*	*e*	*e*
2H-SEP50	lamellae	49.9	*e*	*e*	*e*
2Na-SEP50	lamellae	53.1	*e*	*e*	*e*
2Zn-SEP50	lamellae	49.9	*e*	*e*	*e*

[a] Determined from SAXS. The abbreviation hcp refers to the hexagonal-close-packed arrangement for the block microphase. Cyl denotes cylindrical microphase texture. [b] $D = 2\pi/q^*$ for the block microphase. $D_i = 2\pi/q_i^*$ for the ionic microphase. q^* (or q_i^*) is the value of the scattering vector q (or q_i) at the first scattering maximum. [c] Determined using DMTA. [d] Not applicable. [e] Not measured.

likely an increase in the thermodynamic repulsion between the dissimilar blocks of the block copolymer ionomer. The microstructure of a block copolymer is determined by the value of the phase parameter χN, where χ is the interaction parameter and N is the degree of polymerization.[1] As χN increases, the equilibrium block copolymer texture for a specific composition changes from disordered phase → bcc spheres → hcp cylinders → lam.[20] The introduction of charged species into the PS microphase by sulfonation should increase χ and, thus, χN, which, in the case of the *s*M-SEP20, favored the formation of an lam microstructure. χN may also have been influenced by intermolecular ionic aggregation within the PS domains. The ionic interactions behave as physical cross-links, thereby increasing the apparent molecular weight degree of polymerization, N.

Figure 2 shows the SAXS curves for the *s*M-SEPS21 triblock ionomers. The parent SEPS21 triblock copolymer had a texture of hcp cylinders of PS, as evidenced from the values of $q_m/q^* = 1, \sqrt{3}, 2, \ldots$. Note that the characteristic size, D, of the cylinders for the triblock copolymer (see Table 3) is roughly $^1/_2$ that of the cylinders in the diblock copolymer with comparable molecular weight and composition, SEP20. For the triblock copolymer, unlike the diblock copolymer, sulfonation did not transform the texture; cf. Figures 1 and 2. Instead, the SAXS reflections corresponding to the hcp texture broadened, indicating a less ordered microstructure than for the parent block copolymer. The position of the SAXS maxima, and therefore the characteristic spacing, D, in the block microstructure varied slightly for the different sulfonation levels and cations, though there was no definitive relationship with respect to sulfonation level or cation; see Table 3.

Although the *s*M-SEPS21block copolymer ionomers retained a similar hcp texture as the parent SEPS21, the changes in the SAXS curves in Figure 2 upon sulfonation of SEPS21 are qualitatively similar to those observed when a block copolymer approaches a thermally induced ODT.[1,14] At an ODT, the interphase boundaries become diffuse as a consequence of increased

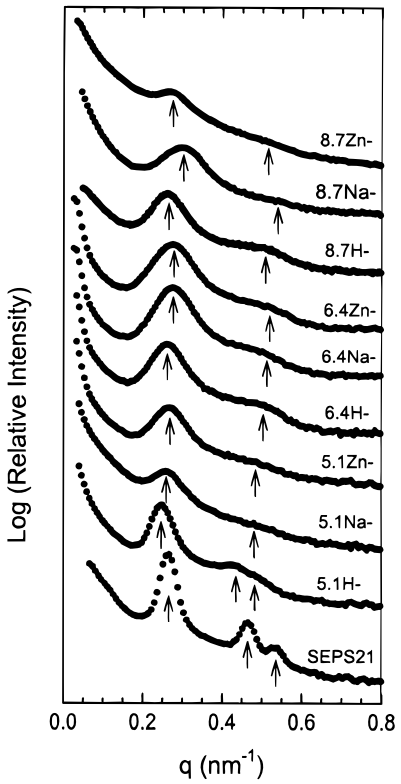

Figure 2. SAXS curves for the block copolymer microphase for SEPS21 and *s*M-SEPS21 ionomers. Vertical arrows indicate maxima of the structure factor, $S(q)$.

Table 3. Microstructure Parameters and Microphase Transition Temperatures for Triblock Copolymer Ionomers

polymer	block microphase texture[a]	D (D_i)[b] (nm)	$T_{g,\,PS}$[c] (°C)	$T_{g,i}$[c] (°C)	T_{ODT}[c] (°C)
SEPS9	llp sph + hcp cyl	21.3	*f*	*d*	80
		~30	*f*	*d*	*e*
17.2H-SEPS9	llp sph	22.6 (5.9)	75	130	*e*
17.2Na-SEPS9	*f*	*f* (6.3)	70	135	278
17.2Zn-SEPS9	*f*	21.2 (5.7)	*f*	130	255
SEPS21	hcp cyl	23.6	102	*d*	157
5.1H-SEPS21	cylinders	25.1	101	120	223
5.1Na-SEPS21	cylinders	24.5	100	120	220
5.1Zn-SEPS21	cylinders	23.9	101	142	257
6.4H-SEPS21	cylinders	23.9	99	137	320
6.4Na-SEPS21	cylinders	22.7	102	145	310
6.4Zn-SEPS21	cylinders	22.7	100	136	305
8.7H-SEPS21	cylinders	24.0	102	140	337
8.7Na-SEPS21	cylinders	21.2	98	197	330
8.7Zn-SEPS21	cylinders	23.9	100	136	330
SEPS50	lamellae	29.0	95	*d*	275
3.6H-SEPS50	lamellae	29.0 (5.9)	100	*f*	331
3.6Na-SEPS50	lamellae	23.3 (5.9)	95	*f*	335
3.6Zn-SEPS50	lamellae	25.2 (5.9)	96	*f*	340

[a] Determined from SAXS. The abbreviations hcp and llp refer to hexagonal-close-packed and liquidlike-packing arrangements for the block microphase, respectively. Sph and cyl denote spherical and cylindrical microphase textures, respectively. [b] $D = 2\pi/q^*$ for the block microphase. $D_i = 2\pi/q_i^*$ for the ionic microphase. q^* (or q_i^*) is the value of the scattering vector q (or q_i) at the first scattering maximum. [c] Determined using DMTA. [d] not applicable. [e] Not measured. [f] Not observed.

microphase mixing. For the block copolymer ionomers, however, the effect is probably kinetic, more so than thermodynamic. The ionic associations within the PS domains decrease mobility of the molecules and thereby hinder the self-assembly of the block microphase. As a

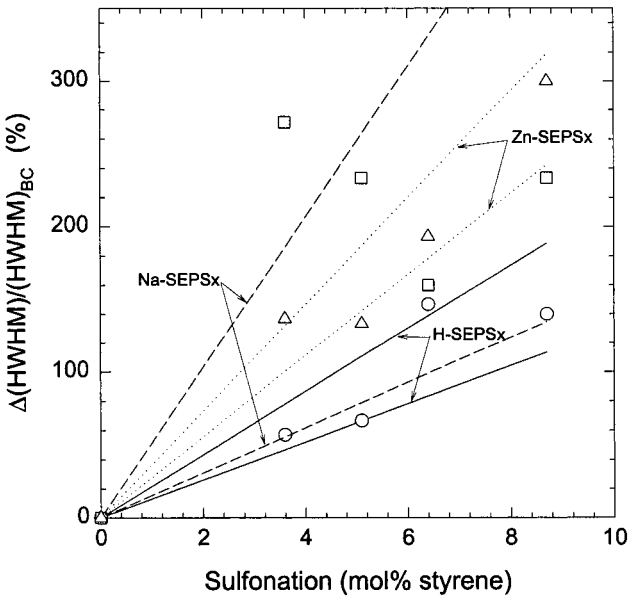

Figure 3. Percentage change in the value of the half-width at half-maximum (hwhm) of the first-order SAXS maximum as a function of sulfonation for *s*M-SEPS*x* ionomers: (○) H-SEPS; (△) Zn-SEPS; (□) Na-SEPS. The lines represent the 95% confidence intervals.

result, an equilibrium microstructure is not easily obtained. One might expect that, for all else equal, the degree of disorder of the block copolymer texture should depend on the strength of the ion−dipole interactions, since the relaxation behavior of the dipolar interactions dictates the local viscosity of the medium. The degree of disorder can be estimated from the half-width at half-maximum (hwhm) of the first-order scattering maximum,[21] and the percent changes of the hwhm for the ionomers, relative to that for the SEPS21 sample, are plotted in Figure 3. The hwhm increased as much as 300% for the sulfonated block copolymers. The metal salts, which had higher viscosities than the free-acid derivative, showed the greater disorder. Generally, for sulfonated polystyrene ionomers, the Na salt derivative has a higher melt viscosity than the corresponding Zn salt derivative, but for the *s*M-SEPS21 ionomers shown in Figure 3, there is no definite trend of the degree of disorder for the two metal salts. For $s = 5.1$ mol %, the Na salt clearly was more disordered, but for $s = 6.4$ and 8.7 mol %, the Zn salt exhibited slightly more disorder.

SAXS curves for the ionomers derived from SEP35 and SEP50 are shown in Figure 4. The values of $q_m/q^* \approx 1, 2, 3, 4, \ldots$ indicated a lam microstructure. Sulfonation had little effect on the position of the SAXS peaks, though the maxima in the SAXS curves of the ionomers, especially the higher order maxima, were much more diffuse. The Na and Zn salts showed considerably poorer resolution of the maxima, and the degree of disorder for the metal salt derivatives was much greater than for the free-acid derivative and the parent block copolymer. For these ionomers, the degree of disorder consistently followed the trend Na salt > Zn salt > free acid > block copolymer, which is consistent with the order of their melt viscosities.

The SAXS results for the 17.2M-SEPS9 ionomers are given in Figure 5. The SAXS curve for the parent SEPS9 block copolymer exhibited a mixed microstructure of PS spheres with liquidlike packing (llp) and coexisting hcp PS cylinders.[17] The first two peaks are first- and second-order diffraction maxima for hcp cylinders. The third

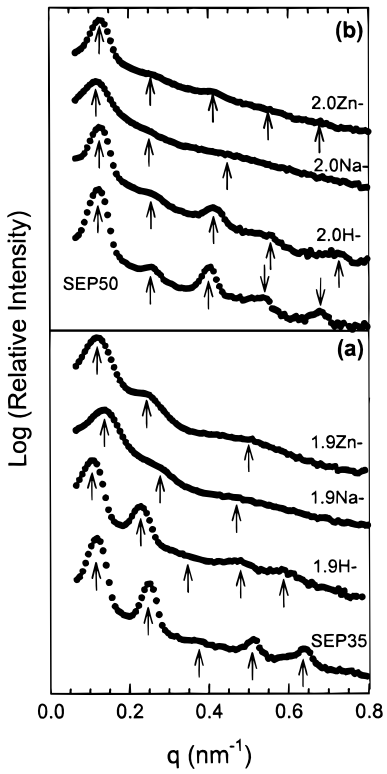

Figure 4. SAXS curves for the block copolymer microphase for (a) SEP35 and *s*1.9-SEP35 ionomers and (b) SEP50 and 2.0M-SEP50 ionomers. Vertical arrows indicate maxima of the structure factor, $S(q)$.

maximum at $q = 0.29$ nm^{-1} is a liquidlike structure factor for PS spheres, which is characterized by the broad form factor at larger angles (marked by the slanted arrow in Figure 5). The first two peaks are absent in the structure factor of the sulfonated polymers, which indicates that the hcp microphase was suppressed in the ionomers. A single, broad maximum in the SAXS structure factor, as well as the particle form factor, persisted for the free-acid derivative, 17.2H-SEPS9, which indicated a texture of llp PS spheres in that material. For the 17.2Na-SEPS9 and 17.2Zn-SEPS9 ionomers, the low-angle peak in the structure factor was very poorly developed, and the particle form factor was not resolved. This indicates that the mesophase texture in those salts was poorly defined and was not unambiguously determined from the SAXS data, though it was probably llp spheres.

Ionic Microstructure. The SAXS curves for the 17.2Na-SEPS9 and 17.2Zn-SEPS9 ionomers in Figure 5 also showed a new peak at $q \approx 1$ nm^{-1} (see bold, vertical arrows) that we attribute to the ionic aggregation in the sulfonated PS phase. The inset to Figure 5 shows the SAXS curves for the three 17.2M-SEPS9 samples measured using a shorter sample geometry (i.e., SDD = 0.474 m) and with the intensity weighted by q^2 to provide better resolution of the ionic peak. Earlier work[14] with sulfonated-SEBS block copolymer ionomers indicated that the morphology of the ionic microphase may be described by a modified hard-sphere cluster model,[22] for which the SAXS ionic peak arises from interaggregate interference. Accordingly, the interaggregate distance between the ionic domains within the spherical PS microdomains, D_i, calculated from Bragg's law, $D_i = 2\pi/q_i^*$, where q_i^* was the value of q at the maximum for the ionic peak, was ca. 6 nm for

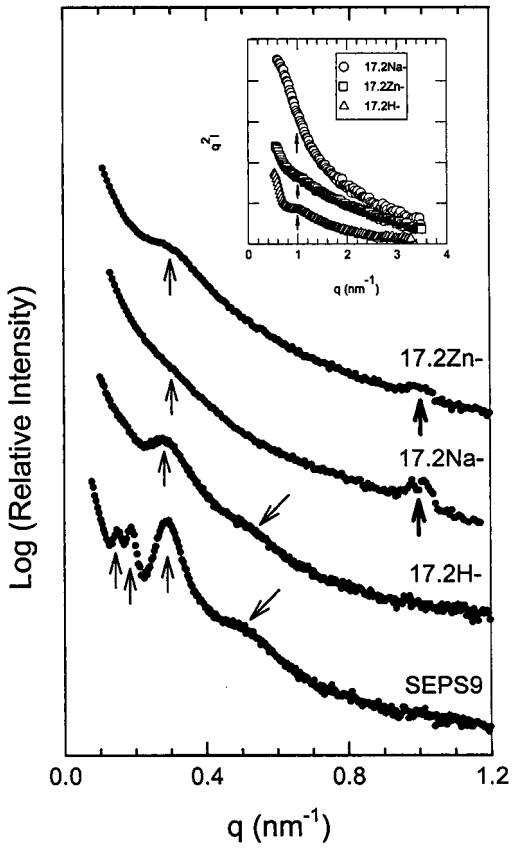

Figure 5. SAXS curves for the block copolymer microphase for SEPS9 and 17.2M-SEPS9 ionomers. Vertical arrows indicate maxima of the structure factor, $S(q)$. Bold arrows and diagonal arrows indicate the ionic peak and particle shape factor, $P(q)$, respectively. The inset shows the SAXS curves for the ionic microstructure.

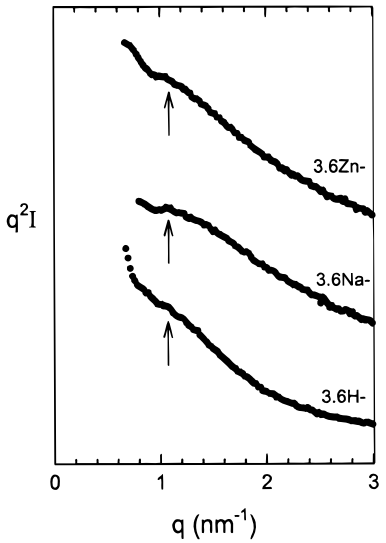

Figure 6. SAXS curve for the ionic microphase for 17.2M-SEPS9 ionomers. The vertical arrows indicate the ionic peak.

the ionomers. That distance is about 1.5−2 times larger than what is typically observed in sulfonated polystyrene ionomers[22] and what was reported[14] for the sulfonated-SEBS block copolymer ionomers.

An ionic peak was also observed in the SAXS data for the 3.6M-SEPS50 block copolymer ionomers (see Figure 6), which had a lam block texture. The peak was located at $q_i^* = 1.06$ nm^{-1} for each of the three salts, which corresponds to $D_i = 5.9$ nm. An ionic peak was not observed in the SAXS data of any of the other ionomers studied here, which is probably a consequence of poor scattering contrast due to the low concentration of the sulfonate species and the poorly developed block microstructure. Evidence for an ion-rich microphase in most of the ionomers, however, was found in the DMTA data that are discussed in the next section.

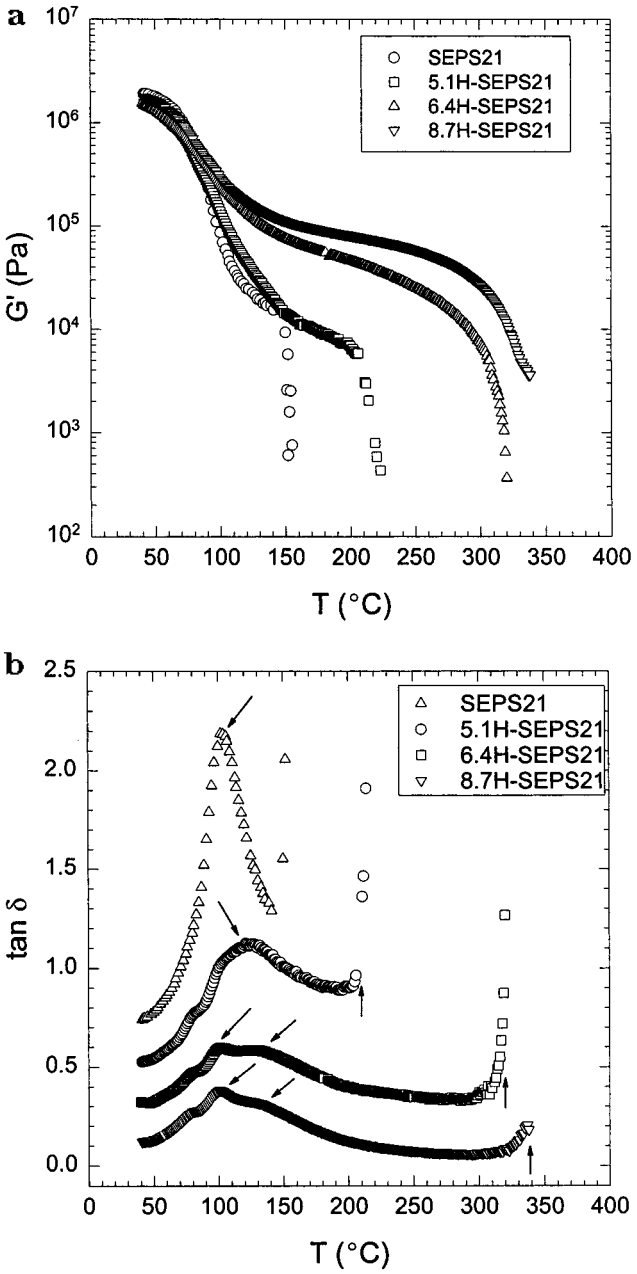

Figure 7. (a) G' and (b) tan δ vs temperature for SEPS21 and sH-SEPS21 ionomers ($f = 0.1$ Hz). Vertical arrows indicate T_{ODT} and diagonal arrows indicate T_g and T_{gi}.

DMTA Results. The effect of sulfonation on the viscoelastic behavior of SEPS21 is shown for the free-acid derivatives in Figure 7. Sulfonation greatly enhances the high-temperature modulus of a block copolymer. A rubberlike plateau develops above the T_g of the PS microdomains, where viscous flow occurs for the parent block copolymer. For the free-acid derivatives, the rubberlike behavior is due to the development of physical cross-links from hydrogen bonding of the sulfonic acid groups, and the enhancement of the rubbery modulus with increasing sulfonation is due to an increase in the "cross-link" density.

The ODT for the block microphase is distinguished by the high-temperature discontinuity in the dynamic modulus, G',[1,17] in Figure 7a. T_{ODT} for *s*H-SEPS21 increases with increasing sulfonation from 157 °C for the parent block copolymer to 257 °C for 5.1H-SEPS and to over 300 °C for a sulfonation level of 6.4 mol % and greater. (Note that caution should be exercised in assigning disordering transitions at such high temperatures, because polymer decomposition may also become significant at such temperatures.) Previous work[16] on sulfonated SEBS block copolymer ionomers indicated that the T_{ODT} of the block microphase is inhibited by the ionic aggregates; i.e., the ODT must be preceded by dissociation of the ionic aggregates, and the temperature of the order−disorder transition of the ionic aggregates may be lower than or equal to T_{ODT}.[16] The T_{ODT} results for the different block copolymer ionomers are tabulated in Tables 2 and 3.

Microphase transitions may also be determined, and in some cases may be more easily resolved, from tan δ vs temperature data.[17] Figure 7b shows the tan δ data for the *s*H-SEPS21 polymers. The vertical arrows denote T_{ODT}, and those values are consistent with the values measured from the G' data. The peak in tan δ, at ca. 100 °C for the SEPS21 and the sulfonated polymers, corresponds to the glass transition of the block-PS microdomains. The tan δ peak at higher temperature probably corresponds to a glass transition of a microphase separated sulfonated polystyrene (SPS) phase, T_{gi}. The transition of that microphase increased from 120 to 140 °C as the sulfonation level for the *s*H-SEPS21 increased from 5.1 to 8.7 mol %. DMTA data for the Na-SEPS21 derivatives are shown in Figure 8. In general, the data are similar to those for the free-acid derivatives, except that the T_{gi} for the Na-SPS microphase was higher than that for the H-SPS microphase. The choice of the cation, however, had little effect on the T_{ODT}.

The DMTA data for the free acid and sodium and zinc salts of 6.4M-SEPS21 are compared in Figure 9. As with the free-acid derivatives, the addition of metal sulfonate groups to the block copolymer gives rise to a distinct rubbery plateaulike region above the T_g of PS microdomains. In contrast, the parent block copolymer exhibits viscous flow at ca. 150 °C, which is coincident with the ODT. The G' data for the three ionomers (Figure 9a) are similar, though 6.4H-SEPS21 had a higher modulus above T_g than did the two metal salts. That result may be due to differences in the microstructure developed during preparation of the samples; the SAXS data indicated better development of the order in the block texture for the free-acid derivatives. The equivalence, or superiority, of the free-acid derivative in stiffening the polymer above T_g was surprising in that for random copolymer ionomers, e.g., M-SPS, the modulus of the metal salts is usually higher than that of the free-acid and viscous flow is suppressed to higher temperatures for the salts. In the case of the block copolymer ionomers, it appears that the strength of the physical cross-link provided by association of the sulfonate groups is less important than the incidence of the cross-link itself. That is, even though the dipole−dipole associations provided by the metal sulfonates are expected to provide stronger and more temperature-resistant physical cross-links than hydrogen bonding of the sulfonic acid groups, their influence on the modulus and ODT is no different than that of the free acid. The tan δ data in Figure 9b show a T_g for the PS microdomains at about 100 °C for the parent SEPS21 and the three 6.4M-SEPS21 ionomers. The ionomers also exhibit a second tan δ peak above T_g, which, based on the elevation of T_g with increasing sulfonation in SPS ionomers,[22] is believed to be due to a T_g of an SPS microphase, i.e., T_{gi}. T_{gi} for the metal salts was higher than for the free-acid derivative.

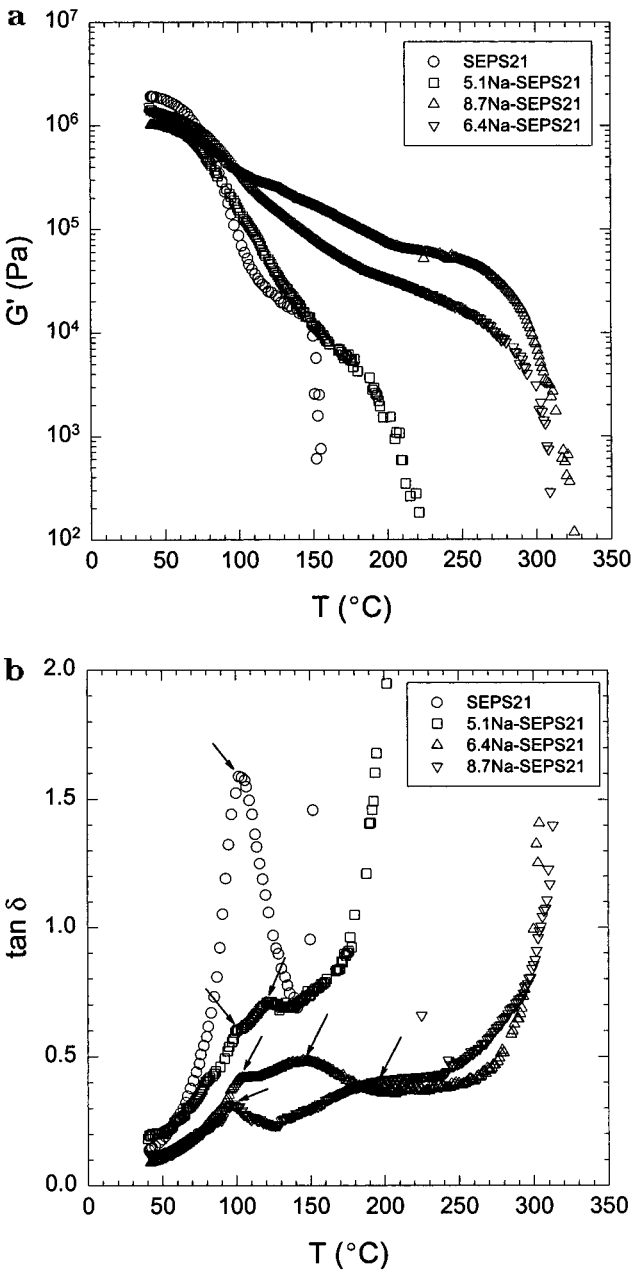

Figure 8. (a) G' and (b) tan δ vs temperature for SEPS21 and sNa-SEPS21 ionomers (f = 0.1 Hz). Diagonal arrows indicate T_g and T_{gi}.

DMTA data for the 5.5M-SEP20 ionomers are shown in Figure 10. The SEP20 diblock copolymer had a much higher T_{ODT} (325 °C) than that of the triblock copolymer with a similar composition, i.e., SEPS21 (157 °C). Sulfonation provided a large improvement of the rubbery modulus of the block copolymer, which may be attributed to the transition of the texture from hcp to lam (see Figure 1) and to the physical cross-links provided by association of the sulfonic acid or metal sulfonate groups. As with the 6.4M-SEPS21 block copolymer ionomers, the 5.5H-SEP20 derivative had a higher modulus than the two metal salt derivatives,

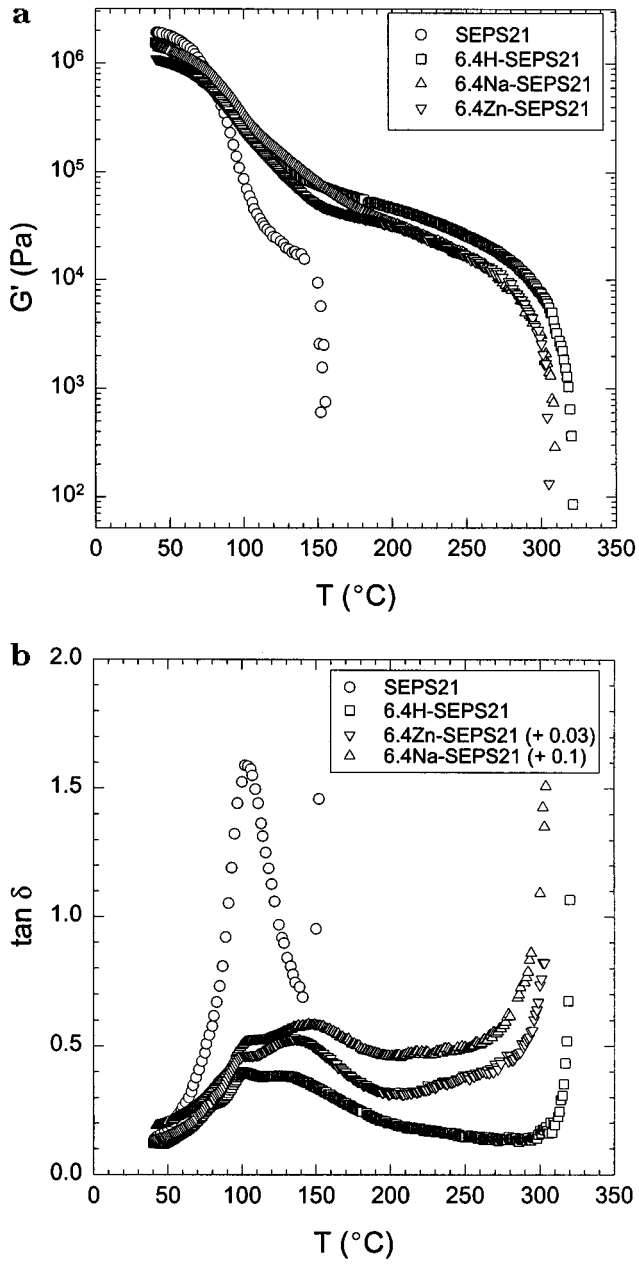

Figure 9. (a) G' and (b) tan δ vs temperature for SEPS21 and sM-SEPS21 ionomers ($f = 0.1$ Hz).

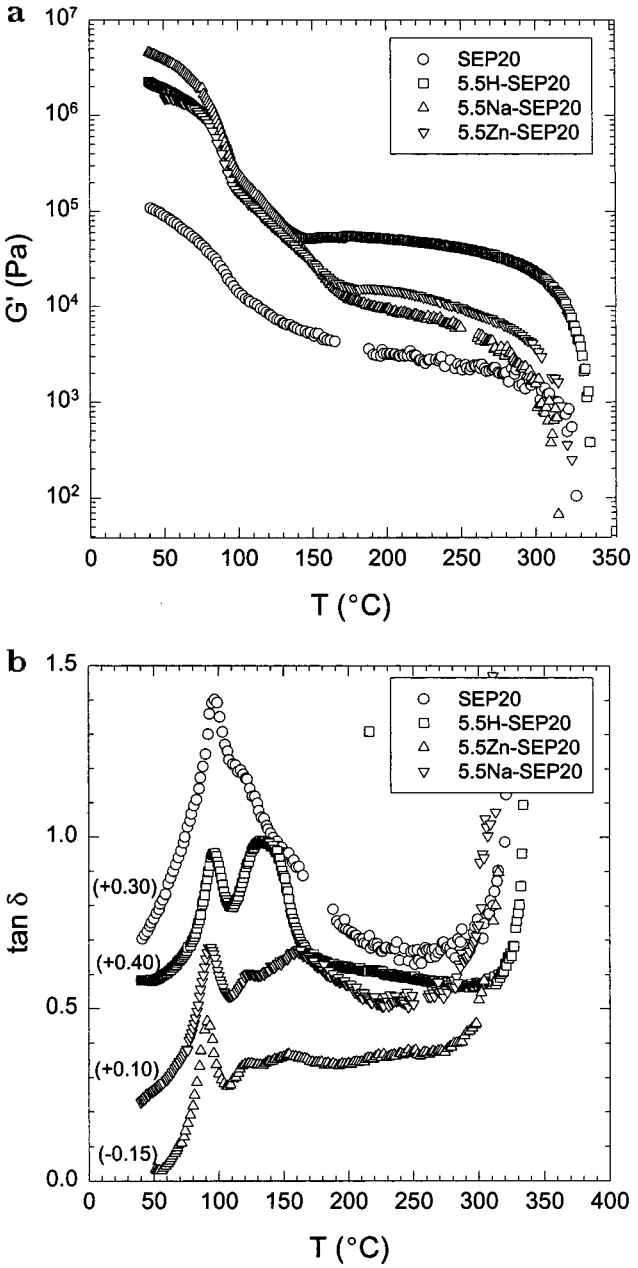

Figure 10. (a) G' and (b) tan δ vs temperature for SEP20 and 5.5M-SEP20 ionomers ($f = 0.1$ Hz). The tan δ data for the different polymers are offset by the value shown in parentheses.

which is probably due to differences in the perfection of the block copolymer microstructure. In fact, the SAXS data in Figure 1 indicate that the block copolymer texture of the free-acid derivative is better developed than for the Zn salt, which is better developed than for the Na salt. The magnitude of G' correlates qualitatively with the SAXS results, in that the modulus decreases with cation on the order of $H^+ > Zn^{2+} > Na^+$. Little difference was observed between the T_{ODT} of the different ionomers with that of the parent polymer; however because the polymers are very sensitive to degradation at temperatures in excess of 300 °C, it was difficult to make accurate measurements of T_{ODT} for these polymers. The T_g of the PS phase, $T_{g,\,PS}$, was ca. 95 °C, and $T_{g,\,I}$ was ca. 150 and 160 °C for the Zn salt and Na salt, respectively. The metal salts also exhibited a small tan δ peak at ca. 120 °C. The origin of that feature is unclear, though the tan δ associated with T_g of the parent block copolymer had a shoulder near 120 °C.

As was discussed earlier in this paper, the ODT of the block copolymer ionomers must be preceded by disordering of the ionic microphase. Because the ionic aggregates in ionomers can persist to very high temperatures,[23] the development of the ionic microphase effectively shifts T_{ODT} to higher temperatures. This is most apparent for the ionomers based on the triblock copolymers, which had T_{ODT}'s that were at relatively low temperatures (see Table 3). The T_{ODT} for the diblock copolymers were near or above 300 °C, where polymer degradation is a significant problem, so that detection of the T_{ODT} is not unambiguous. That is, the materials may degrade before the true T_{ODT} is reached.

The T_{ODT} for the diblock copolymers and their ionomers are plotted in Figure 11 as a function of N_S, the average number of sulfonate groups per chain. T_{ODT} increases with increasing sulfonation and is relatively insensitive to the cation used. The main effect of the

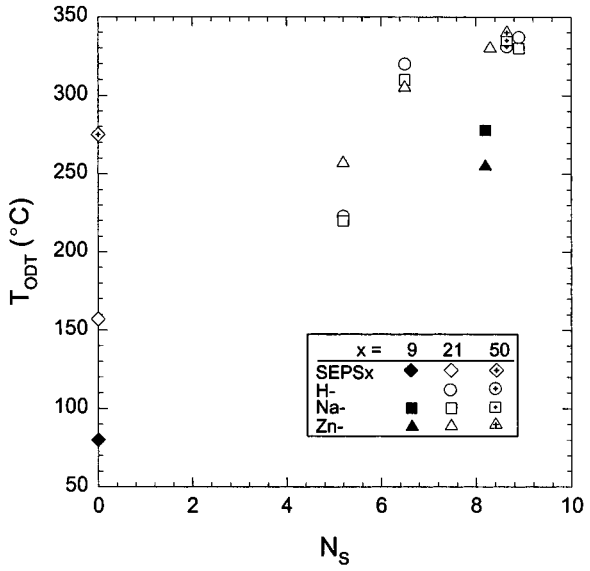

Figure 11. T_{ODT} vs N_S for *s*M-SEPS50, *s*M-SEPS21, and *s*M-SEPS9 ionomers.

block copolymer microstructure (i.e., as the texture changes from spherical (SEPS9) to cylindrical (SEPS21) to lamellar (SEPS50)) is to shift the T_{ODT} to higher temperature. Although the data are limited, it appears that the percent increase of T_{ODT} from sulfonation is similar for the M-SEPS9 and M-SEPS21 ionomers; i.e., $\Delta T_{ODT}/\Delta N_S$ were comparable. The relationship for the lamellar morphology ionomers, M-SEPS50, appeared to be weaker. However, the T_{ODT} for the parent SEPS50 was already close to 300 °C, and because of polymer degradation there is considerable uncertainty in the values of T_{ODT} for those ionomers. Without temperature-resolved SAXS data, we cannot assign a temperature for the order−disorder transition of the ionic domains, $T_{ODT,i}$. However, N_S essentially represents a composition of the ionic microphase, and as such one might expect that $T_{ODT,i}$ should correlate with N_S. In that context, one might, as a first approximation, let $T_{ODT,i} = T_{ODT}$ for these materials, and in that case, Figure 11 provides a relationship between $T_{ODT,i}$ and sulfonation. That conclusion, however, is only speculation at this point, but it does suggest that further characterization of these kinds of materials may provide some additional insight into the thermodynamic transitions in ionomers.

Conclusions

Sulfonation of the polystyrene blocks of a styrene−rubber block copolymer greatly enhances the high-temperature modulus as a consequence of the development of a physical cross-linked network due to association of the sulfonate groups. These intermolecular associations hinder the self-assembly of the block copolymer microstructure, though for the most part, the mesophase texture of the parent block copolymer is qualitatively preserved in the block copolymer ionomer. Where the composition of the block copolymer is close to a transition between mesophase textures, sulfonation can induce such a transition, presumably due to an increase in the χ-interaction parameter between the dissimilar blocks. A second microphase forms in the block copolymer due to microphase separation of ion-rich aggregates, similar to that in random copolymer ionomers. The characteristic size scale determined from SAXS for the ionic microstructure (~6 nm) is much smaller than that of the block copolymer microstructure (~ 20−50 nm).

The ionic microphase perturbs the thermal stability of the block copolymer microstructure. The latter cannot undergo an order−disorder transition until the ionic microstructure disorders. As a consequence, T_{ODT} is greatly enhanced for the block copolymer ionomers compared with the parent block copolymer. The T_{ODT} is relatively insensitive to the cation used (H, Na, or Zn) but increases as the number of sulfonate groups per chain increases.

Acknowledgment. R.A.W. and S.M. are grateful to the Polymer Program (Grant DMR 9712194) and the International Programs Division (Grant INT-9216859) of the National Science Foundation for support of this research. C.E.W. acknowledges support from CNRS through an accord de cooperation CNRS/NSF. We also thank Dr. Dorab Bhagwagar and Dr. Pierre Lesieur for their assistance in collecting the SAXS data.

References and Notes

(1) Bates, F. S.; Fredrickson, G. H. *Annu. Rev. Phys. Chem.* **1990**, *41*, 525.
(2) Bates, F. S.; Schulz, M. F.; Khandpur, A. K.; Förster, S.; Rosedale, J. H.; Almdal, K.; Mortensen, K. *Faraday Discuss. Chem. Soc.* **1994**, *98*, 7.
(3) Hajduk, D. A.; Gruner, S. M.; Rangarajan, P.; Register, R. A.; Fetters, L. J.; Honeker, C.; Albalak, R. J.; Thomas, E. L. *Macromolecules* **1994**, *27*, 490.
(4) Eisenberg, A.; King, M. *Ion-Containing Polymers*; Academic Press: New York, 1977.
(5) Eisenberg, A., Bailey, F. E., Eds. Coulombic Interactions in Macromolecular Systems; *ACS Symp Ser.* **1986**, *No. 302*.
(6) Utracki, L. A., Weiss, R. A., Eds. Multiphase Polymers−Blends and Ionomers; *ACS Symp. Ser.* **1989**, *No. 395*.
(7) Eisenberg, A. *Macromolecules* **1970**, *3*, 147.
(8) Charlier, P.; Jérôme, R.; Teyssié, Ph.; Utracki, L. A. *Macromolecules* **1992**, *25*, 2651.
(9) Nguyen, D.; Williams, C. E.; Eisenberg, A. *Macromolecules* **1994**, *27*, 5090.
(10) Floudas, G.; Fytas, G.; Pispas, S.; Hadjichristidis, N.; Pakula, T.; Khokhlov, A. R. *Macromolecules* **1995**, *28*, 5109.
(11) Weiss, R. A.; Sen, A.; Pottick, L. A.; Willis, C. L. *Polym. Commun.* **1990**, *31*, 220.
(12) Weiss, R. A.; Sen, A.; Pottick, L. A.; Willis, C. L. *Polymer* **1991**, *32*, 1867.
(13) Weiss, R. A.; Sen, A.; Pottick, L. A.; Willis, C. L. *Polymer* **1991**, *32*, 2785.
(14) Lu, X.; Steckle, W. P., Jr.; Weiss, R. A. *Macromolecules* **1993**, *26*, 5876.
(15) Lu, X.; Steckle, W. P., Jr.; Weiss, R. A. *Macromolecules* **1993**, *26*, 6525.
(16) Lu, X.; Steckle, W. P., Jr.; Hsiao, B.; Weiss, R. A. *Macromolecules* **1995**, *28*, 2831.
(17) Mani, S.; Weiss, R. A.; Hahn, S. F.; Williams, C. E.; Cantino, M. E.; Khairallah, L. H. *Polymer* **1998**, *39*, 2023.
(18) Dubuisson, J. M.; Dauvergne, J. M.; Depautex, C.; Vachette, P.; Williams, C. E. *Nucl. Instrum. Methods Phys. Res.* **1986**, *A246*, 636.
(19) Gallot, B. In *Liquid Crystalline Order in Polymers*; Blumstein, A., Ed.; Academic Press: New York, 1978; pp 192−235.
(20) Fredrickson, G. H.; Helfand, E.; Bates, F. S.; Leibler, L. In *Space-Time Organization in Macromolecular Fluids*; Tanaka, F., Doi, M., Ohta, T., Eds.; Springer-Verlag: New York, 1989.
(21) Sakamoto, N.; Hashimoto, T. *Macromolecules* **1995**, *28*, 6825.
(22) Yarusso, D. J.; Cooper, S. L. *Macromolecules* **1983**, *16*, 1871.
(23) Fitzgerald, J. J.; Weiss, R. A. *J. Macromol. Sci., Rev. Macromol. Chem. Phys.* **1988**, *C28* (l), 99.

MA9900986